AMERICAN SOCIETY FOR MICROBIOLOGY | Infection and Immunity®

MOLECULAR PATHOGENESIS

Cyclic di-GMP Regulates the Type III Secretion System and Virulence in *Bordetella bronchiseptica*

María de la Paz Gutierrez,[a] Ting Y. Wong,[b,c] Fredrick Heath Damron,[b,c] Julieta Fernández,[a] Federico Sisti[a]

[a]Instituto de Biotecnología y Biología Molecular-CCT-CONICET-La Plata, Departamento de Ciencias Biológicas, Facultad de Ciencias Exactas, Universidad Nacional de La Plata, La Plata, Argentina

[b]Department of Microbiology, Immunology, and Cell Biology, West Virginia University School of Medicine, Morgantown, West Virginia, USA

[c]Vaccine Development Center at West Virginia University Health Sciences Center, Morgantown, West Virginia, USA

ABSTRACT The second messenger cyclic di-GMP (c-di-GMP) is a ubiquitous molecule in bacteria that regulates diverse phenotypes. Among them, motility and biofilm formation are the most studied. Furthermore, c-di-GMP has been suggested to regulate virulence factors, making it important for pathogenesis. Previously, we reported that c-di-GMP regulates biofilm formation and swimming motility in *Bordetella bronchiseptica*. Here, we present a multi-omics approach for the study of *B. bronchiseptica* strains expressing different cytoplasmic c-di-GMP levels, including transcriptome sequencing (RNA-seq) and shotgun proteomics with label-free quantification. We detected 64 proteins significantly up- or downregulated in either low or high c-di-GMP levels and 358 genes differentially expressed between strains with high c-di-GMP levels and the wild-type strain. Among them, we found genes for stress-related proteins, genes for nitrogen metabolism enzymes, phage-related genes, and virulence factor genes. Interestingly, we observed that a virulence factor like the type III secretion system (TTSS) was regulated by c-di-GMP. *B. bronchiseptica* with high c-di-GMP levels showed significantly lower levels of TTSS components like Bsp22, BopN, and Bcr4. These findings were confirmed by independent methods, such as quantitative reverse transcription-PCR (q-RT-PCR) and Western blotting. Higher intracellular levels of c-di-GMP correlated with an impaired capacity to induce cytotoxicity in a eukaryotic cell *in vitro* and with attenuated virulence in a murine model. This work presents data that support the role that the second messenger c-di-GMP plays in the pathogenesis of *Bordetella*.

KEYWORDS *Bordetella*, c-di-GMP, type III secretion system, label-free proteomics, RNA-seq, immune response

Bordetella bronchiseptica is a Gram-negative respiratory pathogen that infects mammals, including humans. A *B. bronchiseptica* old lineage has been suggested as the common ancestor of the other classical species, *Bordetella pertussis* and *Bordetella parapertussis* (1, 2). *B. pertussis*, a human-adapted pathogen, is the causative agent of whooping cough. Despite high coverage with vaccination, several outbreaks have been recorded in the last 2 decades, prompting the need for a better understanding of the *Bordetella* infection process (3).

B. bronchiseptica possesses a variety of virulence factors required to successfully infect and persist within the host. Adhesins like filamentous hemagglutinin (FHA) and pertactin (PRN) and toxins such as adenylate cyclase toxin (ACT) and the type III secretion system (TTSS) proteins are important for infection (4). The expression of these factors is tightly regulated by a two-component system, BvgAS, the master regulator of *Bordetella* virulence (5). Multifactorial phenotypes like swimming motility and biofilm formation are also regulated by BvgAS (6, 7). Inserted in the inner membrane, BvgS is an active kinase and phosphorylates BvgA, a response regulator of most *Bordetella* virulence factors (8). Although *in vivo* signaling for BvgS is unknown, modulators like low

Editor Igor E. Brodsky, University of Pennsylvania

Address correspondence to Federico Sisti, federico@biol.unlp.edu.ar, or Julieta Fernández, julieta@biol.unlp.edu.ar.

The authors declare no conflict of interest.

Received 7 March 2022
Accepted 28 March 2022

temperatures and millimolar concentrations of magnesium sulfate or nicotinic acid can inhibit BvgS activity *in vitro*, and as a result, the bacteria transition among three phases: the virulent, intermediate, and avirulent phases (9). Virulence factors are absent in the avirulent phase, and the bacteria fail to infect a susceptible host (10).

Since the discovery of the BvgAS system, it has been evident that *Bordetella* pathogenesis is governed mainly by this two-component system. However, in recent years, different authors reported evidence showing how phenotypes involved in infection are also regulated by other signals: an additional sensor kinase, PlrS, is required for *B. bronchiseptica* persistence in the murine lower respiratory tract, RpoE sigma factor regulates ACT expression in *B. pertussis*, and small RNAs are involved in TTSS regulation in *B. pertussis* (11–13). Another two-component system, RisAS, first described as important for resistance to oxidative stress, was recently described in more detail (14). Also, it was reported that the transcriptional regulator BpsR controls loci involved in nicotinic acid degradation and TTSS formation (15). In our laboratory, we showed that the second messenger bis-(3′-5′)-cyclic dimeric GMP (c-di-GMP) regulates biofilm formation and swimming motility in *B. bronchiseptica* (16). When intracellular c-di-GMP concentration is above basal levels, biofilm formation is enhanced and motility is repressed (16, 17). c-di-GMP is a bacterial second messenger known to regulate a variety of cellular processes like biofilm formation, motility, and virulence in many bacteria (18). Intracellular c-di-GMP concentration is regulated by diguanylate cyclases (DGCs) and phosphodiesterases (PDEs), whose activities can respond to different signals. Proteins with DGC activity contain a GGDEF domain, and PDEs contain either an EAL or an HD-GyP domain. Frequently, a sensor and/or regulatory domain is present at the N portion of the enzyme. In accordance with the diversity of signals that modulate the c-di-GMP network, bacterial genomes usually encode several proteins with presumable DGC or PDE activity.

Inspection of the *B. bronchiseptica* RB50 annotated genome revealed 10 probable DGCs and four PDEs. Among them, expression of the DGC gene *bdcA* from a plasmid in *B. bronchiseptica* induces high c-di-GMP levels, enhanced biofilm formation, and motility inhibition (16). Furthermore, we observed impaired colonization of mice by a *B. bronchiseptica* strain lacking *bdcA* (17).

In the present work, we first proposed to establish which proteins are regulated by c-di-GMP in *B. bronchiseptica*. To this end, we set high or low c-di-GMP levels by expressing in *B. bronchiseptica* a DGC or a PDE, respectively, and applied both proteomic and transcriptomic approaches. We used *bdcA* to set high c-di-GMP levels and *bb2664*, which codes for a predicted PDE, to obtain a low c-di-GMP concentration in *B. bronchiseptica*.

Applying shotgun proteomics and label-free quantification, we compared cytosolic protein levels from strains with low and high c-di-GMP levels. In addition, the transcriptome of *B. bronchiseptica* with high c-di-GMP levels was compared with that of the wild type.

Importantly, we observed virulence factors downregulated by c-di-GMP. We showed for the first time that TTSS was regulated by c-di-GMP in *B. bronchiseptica*. In particular, Bsp22, a protein secreted by the TTSS, was downregulated in high c-di-GMP levels. In accordance with TTSS downregulation, *B. bronchiseptica* with high c-di-GMP levels exhibited attenuated virulence in the murine infection model. Although bacteria with artificially high c-di-GMP levels colonized the upper and lower respiratory tracts, the immune response was milder than that developed by mice infected with wild-type bacteria. These results highlight the second messenger c-di-GMP as part of the virulence factor regulation network in *B. bronchiseptica*.

RESULTS

BB2664 is an active phosphodiesterase. To obtain a low c-di-GMP concentration in *B. bronchiseptica*, we chose one of the four putative proteins that contain EAL domains (BB2664) in *B. bronchiseptica*. The primary sequence of BB2664 predicts a cytosolic protein with REC (*cheY*-homologous receiver domain) and EAL domains at the N and C termini,

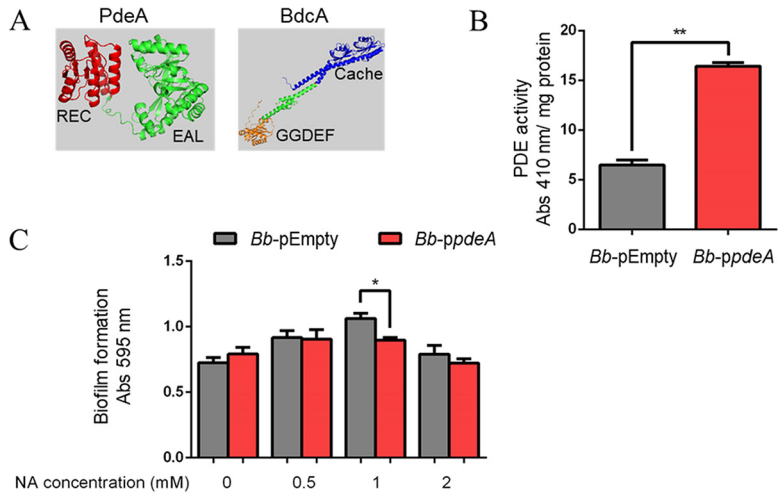

FIG 1 BB2664 (PdeA) exhibits phosphodiesterase activity. (A) AlphaFold prediction structure for BB2664 (PdeA) and BdcA. (B) PDE activity in crude cell extracts of *Bb*-p*pdeA* and *Bb*-pEmpty, using the substrate bis-*p*NPP. The graph shows absorbance (410 nm). The results are based on two biologically independent replicates. **, $P < 0.01$. (C) Biofilm formation by *Bb*-p*pdeA*. Biofilm was allowed to form in U-bottom wells for 24 h and stained with crystal violet (CV) solution. Quantification was conducted by dissolving CV in acetic acid solution and measured absorbance (595 nm). The results are based on three biologically independent replicates. *, $P < 0.01$.

respectively (Fig. 1A). This REC-EAL architecture has been observed in other active PDEs (19). We cloned *bb2664* from *B. bronchiseptica* 9.73 into the pBBR1MCS-5-p*nptII* plasmid downstream of the promoter of *nptII*, to obtain pBBR1MCS-5-p*nptII-bb2664* (p*pdeA*). The presence of a strong and independent promoter upstream of *bb2664* guaranteed its constitutive expression. The plasmid was introduced into wild-type *B. bronchiseptica* by biparental conjugation. Lysates from a *B. bronchiseptica* strain with p*pdeA* (*Bb*-p*pdeA*) were evaluated for PDE activity using the synthetic substrate bis-(*p*-nitrophenyl) phosphate (bis-*p*NPP) (20). Previously, it was shown that EAL domain proteins which were active against c-di-GMP were also active against bis-*p*NPP (21). The reaction product was determined by measuring the absorbance at 410 nm and compared to samples from *B. bronchiseptica* strains harboring an empty plasmid (*Bb*-pEmpty). A significant increase in absorbance was detected in *Bb*-p*pdeA*, indicating the presence of an active PDE domain in this strain (Fig. 1B). From these data, we concluded that BB2664 has PDE activity and therefore propose naming the *bb2664* locus *pdeA* (phosphodiesterase A).

We hypothesized that if PdeA is an active PDE, expression of *pdeA* from a plasmid would decrease intracellular levels of c-di-GMP and, therefore, inhibit biofilm formation in *B. bronchiseptica*, as we observed previously with another PDE (16). To test our hypothesis, we evaluated biofilm formation of a *B. bronchiseptica* strain harboring p*pdeA*. As previously described, wild-type *B. bronchiseptica* showed biofilm formation dependent on the two-component system BvgAS. Under laboratory conditions, it is possible to inhibit BvgAS activity with nicotinic acid (NA). Hence, in the presence of NA (over 2 mM), *B. bronchiseptica* presents an avirulent phase with low biofilm formation capacity. In the absence of added NA, BvgAS is active, virulent factors are expressed, and *B. bronchiseptica* shows enhanced biofilm formation. However, maximum levels of biofilm formation are achieved when intermediate concentrations of NA are added (between 0.5 and 1.0 mM), a condition that is named the intermediate phase. In the experiments whose results are presented in Fig. 1C, biofilm formation by the wild-type strain was in the intermediate phase, as described before (16). Expression of *pdeA* from a plasmid did not change biofilm formation in either the virulent or avirulent phase. However, biofilm formation was significantly inhibited in the intermediate virulence phase (1.0 mM nicotinic acid). This phenotype is expected for *B. bronchiseptica* with low c-di-GMP levels (16).

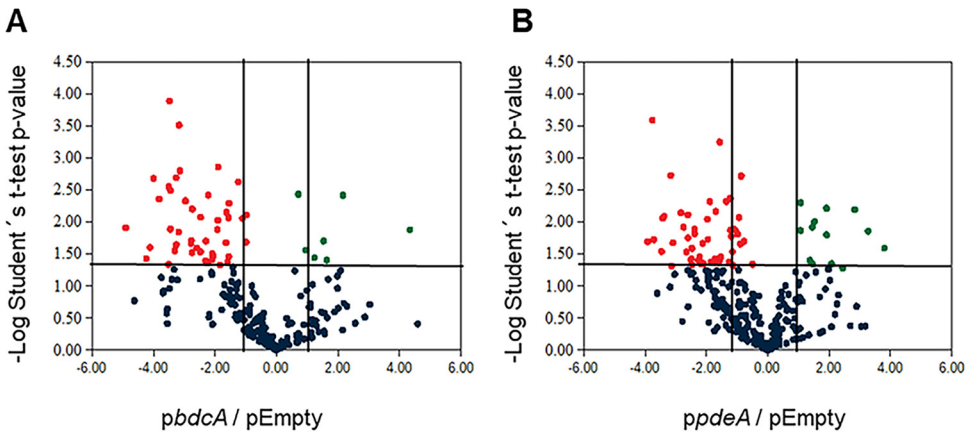

FIG 2 Quantitative analysis of proteins identified in *Bb*-pEmpty and *Bb*-p*bdcA* (A) or *Bb*-p*pdeA* (B) using a shotgun approach. Each plot represents a protein identified in 3 replicates of all conditions, plotted according to its *P* value [$\log_2(P)$] and fold change [$\log_2$(fold change)]. Blue dots represent proteins that meet neither the fold change nor the statistical criteria. Red and green dots correspond to upregulated and downregulated proteins, respectively, satisfying all statistical filters (see Table S1 for protein identity). The horizontal line represents a *P* value of 0.05. The vertical lines show 2- and 0.5-fold changes in protein expression.

Diguanylate cyclase and phosphodiesterase activities regulate protein expression in *B. bronchiseptica*. In previous reports, we established that BdcA is an active DGC (Fig. 1A) (16). High levels of c-di-GMP that correlated with enhanced biofilm formation and motility inhibition were observed in *B. bronchiseptica* when *bdcA* was expressed from a plasmid (16, 17).

To examine the impact of c-di-GMP on the proteome of *B. bronchiseptica*, we performed mass spectrometry on strains overexpressing the DGC BcdA or the PDE PdeA and compared protein expression to that in the parental strain with the empty plasmid. We analyzed the cytosolic fraction of cells by Orbitrap mass spectrometry, and raw data were processed using Perseus software. Spectra from *Bb*-p*bdcA* or *Bb*-p*pdeA* were compared to those of *Bb*-pEmpty. In total, 32,743 spectra were identified with a false discovery rate (FDR) of $<$1% by the Scaffolds Local algorithm.

Overall, we identified 862 different proteins in the three strains. Although samples were obtained from the cytoplasmic fraction, predicted periplasmic and membrane proteins were also identified. We considered for analysis only proteins that were identified in at least two biological replicates of the strains. Due to the shotgun experiment design, the lack of detection of a peptide does not necessarily correlate with absence of a protein. Hence, proteins that were detected in one strain but not in the other were excluded from analysis. We identified 65 proteins with significantly different fold change (FC) in expression relative to the wild-type strain (Fig. 2; also, see Table S1 and Fig. S1 at http://sedici.unlp.edu.ar/handle/10915/135429). In Fig. 2, volcano plots for strains *Bb*-p*bdcA* and *Bb*-p*pdeA* compared to *Bb*-pEmpty are shown. Next, we detail the proteins that were significantly regulated by c-di-GMP.

Proteins that are regulated in *B. bronchiseptica* with high levels of c-di-GMP. *B. bronchiseptica* with p*bdcA* plasmid, with high c-di-GMP levels, showed five proteins that were significantly upregulated. Among them, BB2270 and BB3029 were annotated as putative secreted proteins, with FC of 3.1 and 2.4, respectively. The acetolactate synthase IlvI (BB3887) was surprisingly upregulated with a FC of 20.2. This protein, also known as acetohydroxy acid synthase (AHAS), is the key enzyme involved in the biosynthesis of branched-chain amino acids in bacteria. In a biofilm-versus-planktonic-growth microarray study performed in *B. bronchiseptica* RB50, *bb3887* was shown to be significantly more expressed at 12 h in biofilm-forming bacteria (22).

On the other hand, we observed several groups of proteins downregulated in the strain with high c-di-GMP levels (Table S1; Fig. 2). A group of proteins is predicted to be involved in nitrogen metabolism, and three of them are involved in amino acid synthesis (BB0431 [IlvD], BB2954 [GlnA], and BB0068 [LysA]). Interestingly, we identified two enzymes

described in the conversion of ornithine from glutamate (ArgJ and ArgC) that were downregulated under this condition. Also, BB2658 (GadA), which catalyzes the first step in the conversion of glutamate to succinate, is downregulated in *B. bronchiseptica* with high c-di-GMP levels (FC, 30.1).

Overall, it appears that when c-di-GMP levels were high, glutamate usage as carbon source was inhibited. It is important to note that glutamate is the major carbon source present in the culture medium (Stainer-Scholte medium) (23).

In addition, we found significant differences in three proteins involved in nucleotide metabolism: NadC, BB0845, and BB0957. The first one is a quinolinate phosphoribosyltransferase involved in the quinolinate salvage pathway and was 16 times more abundant in wild-type *B. bronchiseptica* than in *Bb*-p*bdcA*. BB0845 and BB0957 are involved in pyrimidine metabolism according to KEGG pathway prediction; both were downregulated (FC of 9.1 and 9.6, respectively) at high c-di-GMP levels, suggesting downregulation of pyrimidine synthesis in this situation. Decreased expression of pyrimidine synthesis enzymes may be a result of the imbalance in the bacterial nucleotide pool caused by the artificially high c-di-GMP production.

Interestingly, a group of proteins previously described in other bacteria as important for different stress responses was downregulated in *Bb*-p*bdcA*: AhpC, DnaK, and BB4283 (FC of 9.0, 2.9, and 6.8, respectively). BB4283 is a homologue of *Escherichia coli* OsmC, an osmotically inducible protein that has been related to oxidative stress (24). The relationship between oxidative stress and c-di-GMP was described previously (25, 26).

Additionally, *B. bronchiseptica* expressing *bdcA* presented lower levels of SecB and DegP than the wild-type strain. DegP and SecB are involved in the translocation of FHA, an adhesin involved in pathogenesis and biofilm formation, across the cytoplasmic membrane (27).

Proteins that are regulated in *B. bronchiseptica* with low levels of c-di-GMP. Proteomic results from *B. bronchiseptica* strain with low c-di-GMP levels also showed differences from the wild-type strain. We found 29 proteins differently expressed in *Bb*-p*pdeA* compared to *Bb*-pEmpty (Table S1; Fig. 2), most of them downregulated (72%). Among them, two proteins, the putative bacterioferritin BB2881 and the enolase BB3703, were described as being involved in oxidative stress responses (FC of 5.6 and 3.0, respectively) in other pathogens (28).

Other proteins downregulated in *Bb*-p*pdeA* compared to the wild type are related to carbon or nitrogen metabolism, such as BB1381 (FC 5.2), a glyceraldehyde-3-phosphate dehydrogenase; BB3792 (FC 4.5), a putative aminotransferase associated with branched-chain amino acid biosynthesis or degradation; and BB4614 (FC 13.2), an enoyl coenzyme A (enoyl-CoA) hydratase, probably catalyzing amino acid degradation pathways.

We also found that CtpA is slightly but significantly downregulated in *Bb*-p*pdeA* (FC 2.2). CtpA is a protease required for FHA processing and respiratory infection by *B. bronchiseptica* (29).

The most upregulated protein in *Bb*-p*pdeA* was BB3110. BB3110 protein has an autotransporter superfamily domain at the C terminus, homologue to the domain found in the tracheal colonization factor A (TcfA) and pertactin (PRN) from *B. pertussis*. TcfA is important for aerosol infection in *B. pertussis* but is not produced by *B. parapertussis* or *B. bronchiseptica* (30). The BB3110 N-terminal region has homology to the N-terminal portion of TcfA (35% identity), suggesting that BB3110 may be a TcfA-like protein.

Regarding virulence factors, we also found that BipA, a Bvg-intermediate-phase protein, was downregulated when c-di-GMP was lower than basal levels. BipA was 11-fold more abundant in the wild-type strain than in *Bb*-p*pdeA*, being one of the largest fold changes observed in this comparison. OmpA, an outer membrane protein involved in pathogenesis in other pathogens, was also upregulated (FC, 2.4). Under the same conditions, Bsp22, a type III secretion system effector, was upregulated. Two other proteins upregulated in *Bb*-p*pdeA* and likely to be related to bacterial pathogenesis were BB3931 and KdsA, with FC of 4 and 7, respectively. BB3932 is a putative zinc protease,

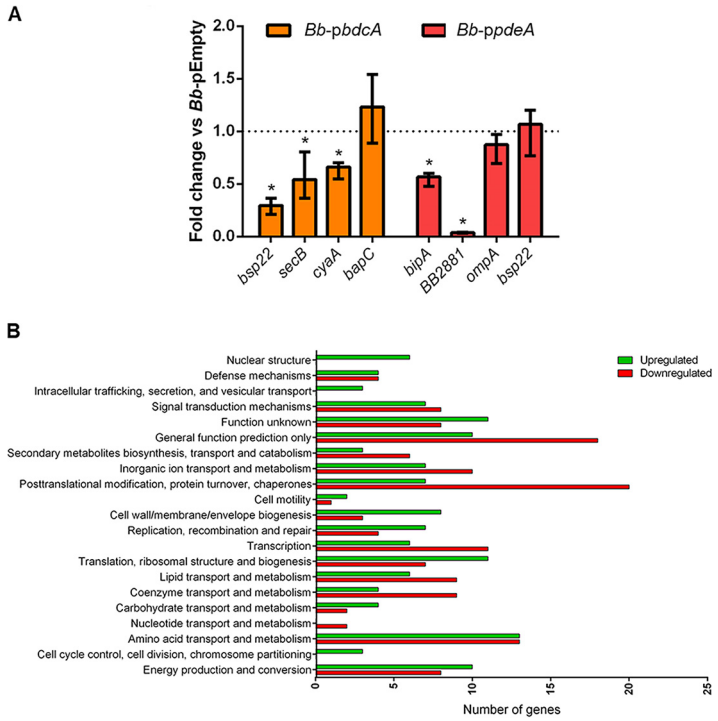

FIG 3 (A) RT-qPCR. mRNA amounts were determined by quantitative real-time PCR. Fold changes were calculated by the $\Delta\Delta C_T$ method using *recA* levels as a control. Mean fold changes of triplicate cultures were compared using Student's paired *t* test (two-tailed distribution), and a *P* value of <0.05 was considered significant. *, $P < 0.05$. (B) Clusters of Orthologous Groups of genes found in the RNA-seq approach. mRNA from *Bb*-pEmpty or *Bb*-p*bdcA* were purified, retrotranscribed to cDNA, and sequenced. Sequences were mapped to the *B. bronchiseptica* RB50 genome and classified according to the ortholog list. Numbers of genes that were upregulated (green bars) or downregulated (red bars) were clustered accordingly to orthologous groups.

while KdsA is a 2-dehydro-3-deoxyphosphooctonate aldolase involved in lipid A synthesis, a component of the lipopolysaccharide, important for pathogenesis (31).

When we compared peptides from *Bb*-p*pdeA* and *Bb*-p*bdcA*, we found additional significant differences (Table S1). Of note, adenylate cyclase (CyaA) and BapC were more abundant in low c-di-GMP levels. Adenylate cyclase is a well described *Bordetella* toxin important for infection progress. BapC has been postulated to be an autotransporter adhesin in *B. pertussis* (32).

To verify whether our results from Orbitrap proteomic agree with mRNA levels, we performed reverse transcription-quantitative PCR (RT-qPCR) of selected genes. Strains were grown and subjected to RNA purification, reverse transcription, and qPCR. Downregulation of *secB* and *cyaA* under high-c-di-GMP conditions determined by RT-qPCR correlated with protein levels (Fig. 3A). Comparison of mRNA levels between the strain expressing *pdeA* and the wild type with empty plasmid showed downregulation of *bipA* and *bb2881*, as observed in the proteomic analysis. In particular, RT-qPCR experiments showed that *bb2881* transcription was strongly inhibited in *Bb*-p*pdeA* (25.8-fold). On the other hand, both *bapC* and *ompA* mRNA levels were indistinguishable in both strains, suggesting that a posttranscriptional mechanism of regulation may be involved.

c-di-GMP-regulation involves transcriptional regulation. c-di-GMP can regulate the expression of proteins at the transcriptional and/or posttranslational level. To further analyze c-di-GMP regulation, we aimed to discover the implications of this second messenger in the transcriptional regulation in *B. bronchiseptica*. Transcriptome sequencing (RNA-seq) analyses were performed to compare transcriptomes of *Bb*-pEmpty to the variant with high c-di-GMP levels. *Bb*-p*bdcA* was chosen because it was the strain showing the highest number of differentially expressed proteins in the proteomic analysis.

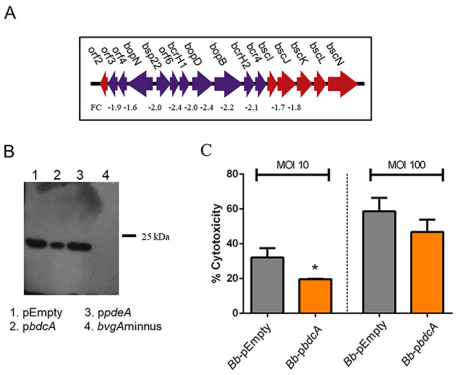

FIG 4 High levels of c-di-GMP regulates the TTSS. (A) Diagram showing the TTSS locus, indicating significant ($P < 0.05$) fold changes. Blue arrows indicate genes for proteins involved in the secretion process. (B) Western blot with anti-Bsp22 antibodies performed on *Bb*-pEmpty, *Bb*-p*bdcA*, *Bb*-p*pdeA*, and *BbbvgA*$^-$ (negative control) supernatant samples. Samples were normalized to cell optical density. Two biologically independent assays were performed. (C) Cytotoxicity assays on J774A.1 macrophages cells. *Bb*-Empty or *Bb*-p*bdcA* was added at the indicated MOI on J774A.1 macrophage monolayers and then incubated for 4 h in 5% CO_2 at 37°C. Cytotoxicity assays were conducted using a Pierce LDH cytotoxicity assay kit, and results were expressed relative to the maximum LDH release control provided by the manufacturer. *, $P < 0.05$ (unpaired one-tailed Student's *t* test).

RNA was isolated from bacteria growing in liquid culture. For each RNA-seq data set, genes with a *P* value of <0.05 (EDGE test) were used for further analysis. Overall, 358 genes were differentially expressed, of which 207 were upregulated and 151 were downregulated in *Bb*-p*bdcA* (Table S2). More than 70 genes were related to transport and metabolism of carbohydrates (6), amino acids (26), nucleotides (2), coenzymes (13), lipids (15), and inorganic ions (17), while about 60 genes were related to transcription (17), translation (18), and posttranslational modifications (27) (Fig. 3B). In addition, a STRING database analysis was performed on the obtained data, and some clusters were discernible, such as phage-, TTSS-, nitrogen-, and stress-related gene clusters (Fig. S2).

Regarding the upregulated genes in *Bb*-p*bdcA*, our analyses revealed more than 60 phage-related genes. Interestingly, some of these genes are upregulated in the first 6 h of biofilm formation by *B. bronchiseptica* (22). Among the downregulated genes, one cluster corresponded to urease genes (*ureC*, *ureF*, *ureE*, *ureG*, and *ureJ*) and others to proteins related to posttranslational modifications or chaperones (*dnaK*, *dnaJ*, *clpB*, *hslU*, *hslV*, and *grpE*). Notably, DnaK downregulation was also observed in proteomic assays with an FC of 2.9 (Table S1).

Interestingly, *cyaB* and *cyaD* were upregulated in *Bb*-p*bdcA*. The gene products of *cyaB* and *cyaD* are known to be necessary for the transport of ACT across the cell envelope and its release into the external medium (33). Also, RseA (BB3751), an anti-sigma factor, was downregulated in *Bb*-p*bdcA*. The absence of RseA in *B. pertussis* liberates RpoE to stimulate *cyaA* expression (12).

Of note, other genes related to c-di-GMP metabolism were differentially regulated between *Bb*-pEmpty and *Bb*-p*bdcA*: *bb2790* and *bb1691*, being putative DGC and PDE genes, respectively, were downregulated in *Bb*-p*bdcA*. The c-di-GMP network is complex, and increasing the amount of an individual DGC or PDE does not necessarily have an impact on the overall levels of c-di-GMP or on a particular phenotype (34, 35).

Both *flhD* and *flhC*, master regulators of motility, were repressed (FC of 4.3 and 2.9, respectively). It is important to note that RNA extractions were performed in cultures under nonmodulating conditions (no motility). Since the mechanism of flagellar inhibition in *B. bronchiseptica* has not been fully described, we speculate that even under this condition, high c-di-GMP levels inhibit basal transcription of the *flhDC* master operon, which might be present in the virulent phase.

We found a remarkable cluster of 10 downregulated genes in *Bb*-p*bdcA* involved in TTSS: *bopN*, *bopD*, *bopB*, *bcr4*, *bcrH2*, *bcrH1*, *bteA*, *bb1614*, *bb1615*, and *bb1618* (Fig. 4A). Furthermore, in accordance with proteomic results, the *bsp22* gene was downregulated

(2.5 times) in *Bb*-p*bdcA*, supporting the idea that c-di-GMP regulates TTSS in *B. bronchiseptica*. We confirmed downregulation of *bsp22* by RT-qPCR; transcription in *Bb*-p*bdcA* was 3.37-fold downregulated compared to *Bb*-pEmpty (Fig. 3A), but no differences in mRNA levels were observed in *Bb*-p*pdeA*. This last result suggests that c-di-GMP is an inhibitor rather than an activator of *bsp22* expression.

c-di-GMP regulates TTSS expression and activity. To confirm that c-di-GMP inhibited *bsp22* expression, we analyzed the presence of Bsp22 in *Bb*-p*bdcA*, *Bb*-p*pdeA*, and wild-type strains' supernatants by immunoblotting. We included the *BbbvgA*$^{-}$ strain as a negative control. Expression of the TTSS is inhibited when the two-component system BvgAS is inactivated (36). As expected, *B. bronchiseptica* showed Bsp22 expression in the virulent phase (Fig. 4B; Fig. S3). We did not observe significant differences in Bsp22 production between the wild-type strain and *Bb*-p*pdeA*. However, consistent with the results shown above, the amount of Bsp22 was reduced in *Bb*-p*bdcA* compared to the wild type.

As it was shown that *B. bronchiseptica* needs a functional TTSS to induce cytotoxicity in mammalian cells, we speculate that if high intracellular levels of c-di-GMP inhibit TTSS in *B. bronchiseptica*, the cytotoxicity should be diminished as well. To assess this issue, we infected J774A.1 cells with either *Bb*-pEmpty or *Bb*-p*bdcA* at multiplicity of infection (MOI) of 10 or 100, and the lactate dehydrogenase (LDH) released was quantified after a 4-h incubation. Bacterial cytotoxicity depended on the MOI assayed, as control strain *Bb*-pEmpty induced about 30% cytotoxicity at an MOI of 10 and 60% cytotoxicity at an MOI of 100 (Fig. 4C), and *Bb*-p*bdcA* was significantly less cytotoxic than *Bb*-pEmpty at an MOI of 10. All these experiments suggest that high intracellular c-di-GMP levels inhibit TTSS-mediated cytotoxic activity on macrophages by downregulating the expression of the secretion system.

***B. bronchiseptica* with high c-di-GMP levels presented attenuated virulence in the murine model.** Considering the downregulation of virulence factors in the *B. bronchiseptica* strain with high c-di-GMP levels, we sought to evaluate the importance of c-di-GMP during *B. bronchiseptica* infection. We infected outbred CD1 mice intranasally with 10^6 CFU of either *Bb*-p*bdcA* or *Bb*-pEmpty, and at 1, 4, and 7 days postinfection, we collected samples and determined bacterial burden in the respiratory tract.

Both *Bb*-pEmpty and *Bb*-p*bdcA* were recovered from the lungs, tracheas, and nasal cavities of infected mice at all time points (Fig. 5). *Bb*-pEmpty presented an infection kinetic already described previously by our laboratory (37). Bacteria were recovered from the three sites analyzed, with a peak of 10^7 CFU in the lungs at day 4 postchallenge. On day 7, two *Bb*-pEmpty-infected mice were found dead; tissues were processed, but CFU were not considered for statistical analysis (gray dots in Fig. 5).

Overall, *Bb*-p*bdcA* showed a typical kinetics of infection in the lungs, although its CFU counts were lower than those for *Bb*-pEmpty, and it also showed impaired growth in the nasal cavity and trachea. Specifically, we recovered statistically 1 to 2 log fewer viable *Bb*-p*bdcA* bacteria from lungs at days 1 and 4 postinfection (Fig. 5A). Also, we recovered 2 log fewer *Bb*-p*bdcA* than *Bb*-pEmpty bacteria from tracheas at day 7 postinfection (Fig. 5B). Regarding bacterial colonization in the nasal cavity, we observed little growth of *Bb*-p*bdcA*, if any, as we recovered a constant number of CFU during the analyzed period (Fig. 5C). Less viable *Bb*-p*bdcA* was recovered from nasal washes 4 days postinfection than *Bb*-p*Empty*. However, this difference was not observed in nasal mucosa-associated lymphoid tissue (NALT) samples (Fig. 5D). Nasal washes contain only bacteria that can be flushed out of the nostrils. On the other hand, NALT samples contain bacteria that remain attached to the epithelium. These data indicate that *Bb-pbdcA* was able to colonize and persist in the respiratory tract of mice but not as efficiently as the wild-type strain. In summary, we observed a decrease in the bacterial burden in the respiratory tract by the *Bb*-p*bdcA* strain compared to *Bb*-p*Empty*.

Infection with *Bb*-p*bdcA* led to fewer infiltrating phagocytes at the site of infection and induced a milder proinflammatory immune response. To characterize the immune response produced by the host infected with *Bb*-p*bdcA*, neutrophil and monocyte populations were studied in blood and lung homogenates by flow cytometry.

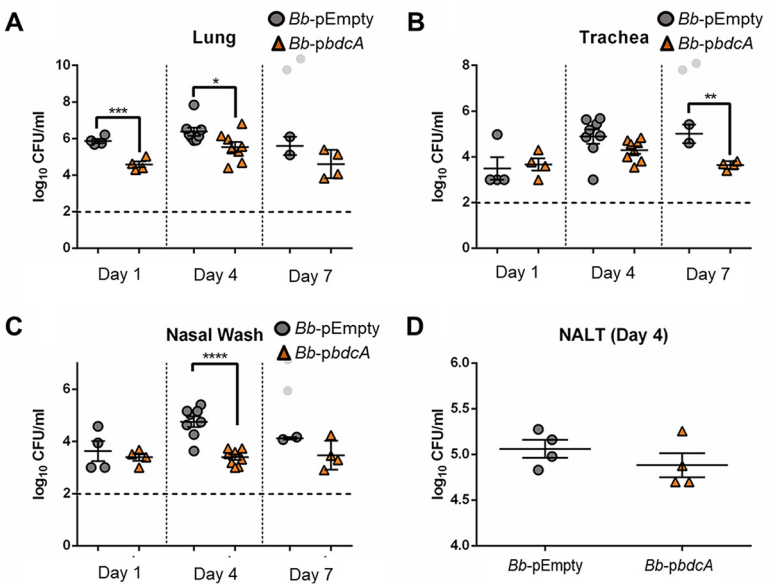

FIG 5 *B. bronchiseptica* with high c-di-GMP levels presented attenuated virulence in the mouse model. Mice were inoculated intranasally with 1×10^6 CFU of either *Bb*-pEmpty or *Bb*-p*bdcA* at 1, 4, and 7 days postinfection, and bacteria were recovered and quantified by serial dilution and colony counting. Bacterial burden was determined in lungs (A), tracheas (B), and nasal wash (C). CFU counts in nasal-associated lymphoid tissue (NALT) samples were determined at day 4 postinfection (D). Each symbol represents data from one mouse. Light gray dots correspond to CFU of mice infected with *Bb*-pEmpty found dead at day 7 and excluded from statistical analysis. Results are means and standard errors of the means (SEM). *, $P \leq 0.05$; **, $P \leq 0.01$; ***, $P \leq 0.001$; ****, $P \leq 0.0001$. *P* values were determined by two-tailed unpaired *t* test.

Overall, both *Bb*-pEmpty and *Bb*-p*bdcA* induced a strong recruitment of neutrophils (Gr-1^{high} CD11b$^+$) and monocytes (Gr-1^{mid} CD11b$^+$) to the lungs at day 1 compared to the control (Fig. 6A and B). However, the number of neutrophils in *Bb*-p*bdcA*-infected lungs was significantly lower (50%) than in *Bb*-pEmpty-infected ones at day 1 postinfection (Fig. 6A). At day 7 postinfection, *Bb*-pEmpty-infected lungs exhibited a 75% increase in neutrophils relative to both *Bb*-p*bdcA*-infected and uninfected lungs (Fig. 6A). Furthermore, while the number of monocytes was similar between mice infected with either strain at day 1, the amount recovered from *Bb*-p*bdcA*-infected lungs was constant and indistinguishable from control lungs throughout the experiment (Fig. 6B). In contrast, wild-type bacteria induced a persistent recruitment of monocytes to the lungs at all time points analyzed, showing values 80% and 60% higher than those in the *Bb*-p*bdcA*-infected lungs at days 4 and 7 postinfection (Fig. 6B).

To simply assess inflammation, we measured the weight of the lungs. *Bb*-pEmpty-infected lungs weighed more than *Bb*-p*bdcA*-infected lungs at day 4 and day 7 postinfection (Fig. S4). Furthermore, blood analyzed by a hematology blood analyzer showed that white blood cell profiles from *Bb*-p*bdcA*-infected mice were similar to those of the uninfected control group at days 4 and 7 (Fig. S5). Regarding neutrophil population detected by flow cytometry in blood samples, a significant increase in *Bb*-pEmpty-infected mice was observed (between 30 and 40%) compared to *Bb*-p*bdcA*-infected ones at the three time points analyzed (Fig. 6C). In summary, mice infected with *Bb*-p*bdcA* showed fewer infiltrating cells recruited to lungs, less inflamed lungs, and a reduction in neutrophil population in blood compared to those infected with *Bb*-pEmpty.

We further analyzed the cytokine response by measuring cytokines in lung homogenates with a Multi-Spot assay (Meso Scale Discovery). We observed that *Bb*-pEmpty induced an increase in the production of several cytokines in the lungs, as expected for a *Bordetella* infection. In contrast, *Bb*-p*bdcA* triggered a milder production of the cytokines analyzed during the 7 days postinfection (Fig. 7). Furthermore, the *Bb*-p*bdcA*-induced cytokine profile was not significantly different from that in nonchallenged mice. The levels of

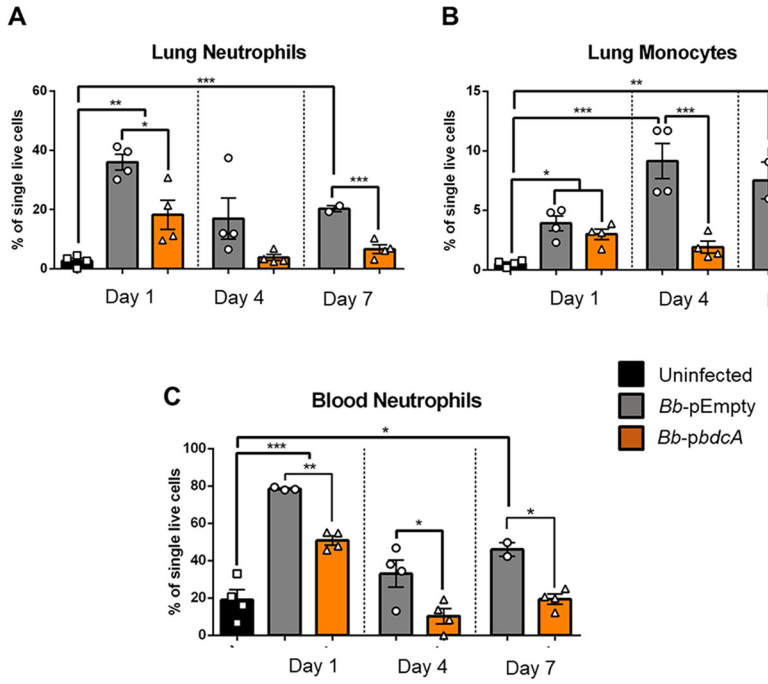

FIG 6 *Bb*-p*bdcA* recruited fewer infiltrating phagocytes to the site of infection. Immune cells were measured by flow cytometry at 1, 4, and 7 days postinfection. Neutrophils were identified as Gr-1^{high} $CD11b^{+}$. Monocytes were identified as Gr-1^{mid} $CD11b^{+}$. (A) Proportion of neutrophils in lung homogenates. (B) Proportion of monocytes in lung homogenates. (C) Proportion of neutrophils in blood. Group comparisons were analyzed by one-way ANOVA followed by Tukey's multiple-comparison test. Each symbol represents data from one mouse. Results are means and SEM. *, $P \leq 0.05$; **, $P \leq 0.01$; ***, $P \leq 0.001$.

the proinflammatory cytokines gamma interferon (IFN-γ) and tumor necrosis factor alpha (TNF-α), associated with a Th-1 profile, were 1 to 2 log higher in *Bb*-pEmpty-infected mice than *Bb*-p*bdcA*-infected ones throughout the experiment (Fig. 7). IL-5, a proinflammatory cytokine associated with a Th-2 profile, was significantly higher in lungs infected with *Bb*-

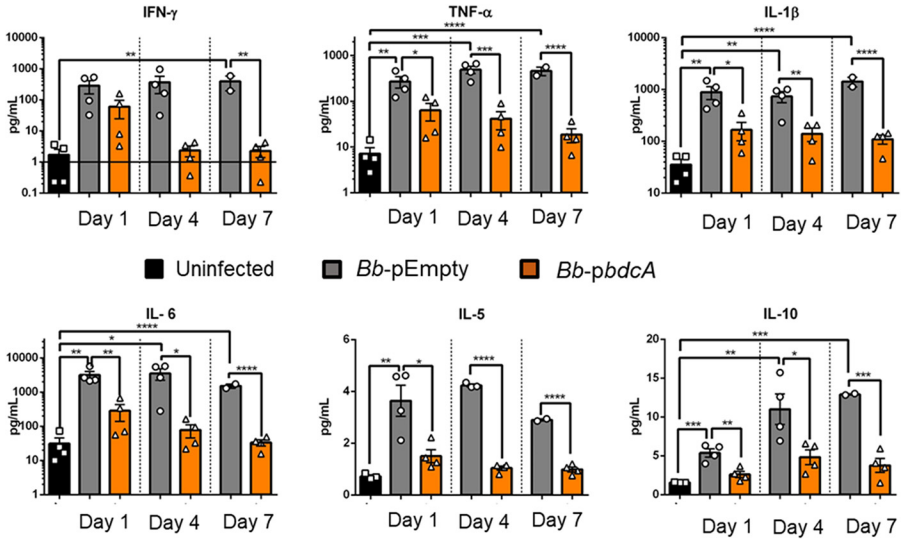

FIG 7 *Bb*-p*bdcA* induced a milder proinflammatory immune response. Murine cytokines were detected in supernatants of lung homogenates at days 1, 4 and 7 postinfection. (A) IFN-γ, (B) TNF-α, (C) IL-1β, (D) IL-6, (E) IL-5, and (F) IL-10 were measured by Meso Scale Discovery's V-plex Plus proinflammatory panel 1 mouse multiplex kit. Group comparisons were analyzed by one-way ANOVA followed by Tukey's multiple-comparison test. Each symbol represents data from one mouse. Results are means and SEM. *, $P \leq 0.05$; **, $P \leq 0.01$; ***, $P \leq 0.001$; ****, $P \leq 0.0001$.

pEmpty than in *Bb*-p*bdcA*-infected ones at days 1, 4, and 7 postinfection (Fig. 7). Also, *Bb*-pEmpty-infected mice exhibited a great increase in the levels of the Th-17-associated cytokines interleukin 1β (IL-1β), IL-6, and IL-10 compared to *Bb*-p*bdcA*-infected mice (Fig. 7). The proinflammatory cytokines IL-1β and IL-6 were about 1 log higher at days 1, 4, and 7 postinfection in lungs infected with *Bb*-pEmpty than those with *Bb*-p*bdcA* (Fig. 7). Interestingly, *Bb*-pEmpty-infected mice showed increases of 50, 55, and 70% in the levels of IL-10 compared to *Bb*-p*bdcA*-infected mice at days 1, 4, and 7 postinfection (Fig. 7). IL-10 is an anti-inflammatory cytokine known to be positively regulated by *Bordetella* TTSS that promotes bacterial colonization (38).

Overall, these data suggest that *B. bronchiseptica* with high c-di-GMP levels fails to induce a strong proinflammatory response.

DISCUSSION

The second messenger c-di-GMP coordinately regulates many phenotypes in different bacteria. In general, the mechanism of regulation involves c-di-GMP binding to a protein. Once it is bound, conformational changes are observed in the protein that elicit a response. When the protein is part of an adhesin regulator system, surface-related phenotypes are involved; when a transcription factor changes its conformation, a different array of genes is expressed. The c-di-GMP network has been extensively studied, and it has been revealed to be complex and intricate. However, different bacteria do not frequently share mechanisms to regulate the same phenotype. *B. bronchiseptica* motility and biofilm formation may be regulated by c-di-GMP by still-unknown mechanisms (16, 17).

In this study, we used shotgun proteomics and RNA sequencing approaches to find proteins involved in c-di-GMP-regulated phenotypes in *B. bronchiseptica*. To artificially manipulate the intracellular c-di-GMP levels, we expressed from a plasmid a gene for either a DGC (*bdcA*) or a PDE (*pdeA*). We described BdcA previously, and in this study, we describe PdeA for the first time (Fig. 1). Consistent with a high number of enzymes that synthetize and degrade c-di-GMP, not all DGCs or PDEs are involved in the regulation of all c-di-GMP-related phenotypes. Therefore, a possible limitation of the present work is that some proteins, regulated by c-di-GMP, are not regulated by BdcA or PdeA. We hypothesized that overexpression of these genes would overcome this possible limitation.

Using shotgun proteomics and label-free quantification, we detected 64 different proteins in *B. bronchiseptica* regulated by differences in the intracellular c-di-GMP concentration. RNA-seq revealed a total of 358 genes differentially expressed between *Bb*-p*bdcA* and *Bb*-pEmpty. Proteins with different expression profiles belong to different groups, such as metabolic proteins, adhesins, virulence factors, chaperones, or shock proteins (Fig. S1), indicating that c-di-GMP can modulate different phenotypes.

High levels of c-di-GMP repressed a group of proteins involved in energy metabolism an average of 6-fold compared to the wild-type strain. Interestingly, NadC is downregulated when the c-di-GMP levels are high. NadC is a quinolinate phosphoribosyltransferase recently described in *Bordetella* as essential for a quinolinate salvage pathway (39). NAD metabolism plays an important role in *B. bronchiseptica* physiology, but *Bordetella* species lack the *nadA* and *nadB* genes needed for *de novo* NAD biosynthesis (39). Therefore, to synthesize NAD, *Bordetella* has at least two salvage pathways, in which the NAD precursor nicotinic acid mononucleotide is made either via NadC or via PncB, a nicotinic acid phosphoribosyltransferase. Our results suggest that under high-c-di-GMP conditions, PncB salvage pathways may be preferred.

Among the proteins that were downregulated in low c-di-GMP levels, we found BB2881, a putative bacterioferritin comigratory protein (BCP). BCPs are members of the peroxiredoxins, thiol-specific antioxidant proteins that play an important role in reactive oxygen species (ROS) detoxification. Label-free quantification showed that BB2881 is downregulated 5.6-fold compared to in the wild-type strain, suggesting that c-di-GMP may be involved in resistance to the host ROS response. The small amount of protein detected

correlates with a very low level of *bb2881* transcription under *pdeA* expression (25-fold compared to wild-type levels, determined by RT-qPCR) (Fig. 3A). Expression of BB2881 appears to be regulated only by c-di-GMP absence: when c-di-GMP levels were high, BB2881 expression was not activated. A hypothesis including a transcription factor inhibited by c-di-GMP can be considered to support these experimental data.

Many virulence factors have been described for *B. bronchiseptica*. When the cytosolic fraction of *Bb*-p*pdeA* or *Bb*-p*bdcA* was analyzed, some virulence factors were upregulated in low c-di-GMP concentrations or vice versa. Specifically, some adhesins were regulated by c-di-GMP levels. We previously showed that a large adhesin, BrtA, is regulated by c-di-GMP, like its homologous system of Lap proteins in *Pseudomonas fluorescens* (37). In this work, we observed in *Bb*-p*bdcA* the downregulation of two proteins involved in filamentous hemagglutinin (FHA) secretion: SecB (BB0295) and DegP (BB3749). DegP is a protease involved in FHA maturation, cleaving the N-terminal portion of FHA (27). Once cleaved, the resulting protein, called the FHA clipped product, is the substrate for another protease, CtpA. Interestingly, CtpA is slightly but significantly downregulated in *Bb*-p*pdeA* (FC, 2.2) under low-c-di-GMP conditions. After CtpA cleaves N-terminal FHA, the adhesin is either released from the bacterial surface or, if the bacteria are grown for extended periods of time, cleaved by another protease, SphB1, to produce mature FHA that is released. Overall, these results suggest that c-di-GMP might be involved in the secretion and detachment of FHA from the bacterial surface, regulating protease activity.

We also observed that another adhesin, BipA, was downregulated in low c-di-GMP concentrations. Regulation of *bipA* by the BvgAS system has been described widely, but its function during infection remains uncertain. Deletion of this protein from *B. bronchiseptica* results in nonsignificant defect during infection in the murine model (40). *Bordetella holmesii* BipA plays an essential role in preventing autoagglutination and promoting biofilm formation indirectly, since BipA is one of the most abundant surface proteins in this *Bordetella* specie (41). Since BipA is an intermediate-phase adhesin and we observed that biofilm formation was diminished in the intermediate phase when *pdeA* was overexpressed, we speculate this may be due to downregulation of adhesins such FHA, BrtA, and BipA in *Bb*-p*pdeA*. Notably, no differences in RNA-seq analysis were observed in *Bb*-p*bdcA* regarding adhesin expression, suggesting a posttranscriptional regulation by c-di-GMP levels or c-di-GMP-related proteins.

The regulation of TTSS by DGCs or PDEs has been described in other pathogens (18, 42–46). The regulation mechanism of TTSS locus expression and posttranscriptional modification of proteins by the c-di-GMP are partially understood. In *Salmonella enterica* serovar Typhimurium and *Pseudomonas* spp., transcriptional and posttranscriptional regulation was described (42–45). Interestingly, the Römling group demonstrated that DGC activity is unnecessary for TTSS activity inhibition in *S. enterica* (42, 43). However, Moscoso et al. (44) concluded after analyzing TTSS activity in different mutants that c-di-GMP levels regulates TTSS in *P. aeruginosa*. Also, Yi and coworkers demonstrated that deletion of a PDE inhibits TTSS expression in *Dickeya dadantii*: while a wild-type PDE restored expression, a null activity mutant did not, suggesting the importance of PDE activity for regulation (46).

Considering that we observed differences in bacteria overexpressing either a DGC or a PDE, we propose that c-di-GMP levels may regulates TTSS activity at the transcriptional level in *B. bronchiseptica*.

One TTSS protein exclusively expressed in *Bordetella* spp. is Bsp22, which is located at the tip of the injectosome. Disruption of *bsp22* affects long-term colonization levels in the tracheas of immunocompetent mice (47). Interestingly, expression of *bsp22* is present in a significant proportion of clinical isolates but not in common laboratory-adapted strains of *B. pertussis* (48). Here, we showed for the first time that *bsp22* expression is downregulated by intracellular c-di-GMP levels. We observed significant downregulation in *bsp22* expression in both proteomic and transcriptomic experiments, and we confirmed these results by Western blotting and RT-qPCR (Fig. 3). We also found that *btc22* is downregulated in the presence of high c-di-GMP levels (FC of 2) (Table S1). Btc22 is a chaperone that influences the secretion and intracellular

stability of Bsp22 (49). Consistent with these results, transcriptomic analysis indicates that the cluster of genes in the TTSS locus is regulated by c-di-GMP. This cluster includes genes that encode extracellular components of the translocation needle, the membrane-penetrating translocon and other secreted apparatus components. This cluster is regulated by the anti-sigma factor BtrA (also called BspR) and BvgS and has been named cluster 4b (50). BtrA binds and antagonizes BtrS, a BvgAS-regulated extracytoplasmic function (ECF) sigma factor. In this study, we demonstrated that high c-di-GMP levels downregulate TTSS transcription and translation. Although *bspR* and *btrS* mRNA were detected in RNA-seq analysis, no significant differences in expression were observed between strains.

Also present in cluster 4b, *bcr4* was downregulated by high c-di-GMP levels. Bcr4 strongly stimulates the production of type III secreted proteins (51).

As previously reported, the *B. bronchiseptica* TTSS is important for virulence and it is required for the induction of macrophage apoptosis *in vitro* (47). We found that c-di-GMP-mediated regulation is important for TTSS-mediated cytotoxicity. *In vitro* experiments with immortalized J774.1 macrophages demonstrated that high c-di-GMP levels correlated with diminished cytotoxicity (Fig. 4D).

Given the importance of TTSS during infection and that of the other virulence factors and phenotypes regulated by c-di-GMP, we decided to further investigate if c-di-GMP regulation plays a key role in *B. bronchiseptica* pathogenesis. The strain with high c-di-GMP levels, *Bb*-p*bdcA*, was able to infect mice, but fewer viable bacteria were recovered from the respiratory tract than with *Bb*-pEmpty-infected mice.

The importance of TTSS in *B. bronchiseptica* infection was previously described. Nagamatsu and coworkers recovered fewer TTSS mutant cells from the lungs of mice 2 and 7 days after infection (38). Also, lower levels of TTSS and *bsp22* mutants were recovered from the tracheas of mice 7 days postinfection in experiments reported by Yuk and coworkers (47). The differences in bacterial colonization that we describe in this work between the wild type and bacteria with high c-di-GMP levels seem to correlate with the infection kinetic of TTSS mutants.

Bb-pEmpty-infected lungs were notably more inflamed than *Bb-pbdcA*-infected ones and exhibited higher levels of infiltrating phagocytes and proinflammatory cytokines (IL-6, IL-5, IL-1β, IFN-γ, and TNF-α), indicating that *Bb*-p*bdcA* triggered a milder immune response than *Bb*-pEmpty.

Interestingly, we observed downregulation of IL-10 secretion in *Bb-pbdcA* infected mice. Low IL-10 levels correlate with results observed in mice infected with a *bopN* mutant (38). BopN is a TTSS factor that, once translocated to the nucleus, downregulates mitogen-activated protein kinases. A BopN-deficient strain was unable to induce IL-10 production in mice, resulting in the elimination of bacteria. Unlike what we observed in *Bb*-p*bdcA* infected mice, absence of BopN stimulates IFN-γ in the lungs of C57BL/6J mice (38). This suggests that IL-10 inhibition by c-di-GMP may be through TTSS regulation, while the second messenger could regulate IFN-γ inhibition by another network. It is well established that disruption of IFN-γ signaling during a murine infection with *B. pertussis* results in a lethal disseminating disease (52). Mice infected with *Bb*-p*bdcA* had lower levels of IFN-γ than the parental strain, but mice were able to control the infection. Our results suggest that *B. bronchiseptica* with artificially high intracellular c-di-GMP levels exhibited mild virulence, resulting in an inability to persist within the host. In conclusion, when the intracellular levels of c-di-GMP were constitutively high, the bacteria were eliminated from the mice, not because the immune response was greater, but probably because the bacteria could not proceed in the infection process. This result is in agreement with other reports for many species where elevated c-di-GMP levels are associated with attenuated virulence. For example, high c-di-GMP levels inhibit *Francisella novicida* virulence in mice and intracellular replication in macrophages (53). Also, in a mouse model of *Brucella melitensis* infection, deletion of all DGCs increases virulence, whereas deletion of all PDEs reduces it (18).

Our results demonstrate that c-di-GMP levels in *B. bronchiseptica* are intimately involved in virulence regulation. High levels of the second messenger inhibit the

TABLE 1 Plasmids and strains used in this work

Plasmid or strain	Description	Reference
Plasmids		
pBBR1MCS-5-*npt*II	pBBR1MCS-5 with *npt*II promotor	16
p*bdcA*	pBBR1MCS-5-*npt*II with *bdcA* downstream promotor nptII	16
p*pdeA*	pBBR1MCS-5-*npt*II with BB2664 (*pdeA*) downstream promotor nptII	This work
B. bronchiseptica strains		
*Bb*WT	Wild type strain; 9.73H$^+$ Sm^r	65
BbbvgA$^-$	*Bb*9.73H$^+$ strain with the gene *bvgA* interrupted by pK18mob insertion	16
Bb-pEmpty	*Bb*9.73H$^+$ wild-type strain with pBBR1MCS-5-*npt*II	16
Bb-p*bdcA*	*Bb*9.73H$^+$ wild-type strain with p*bdcA*	16
Bb-p*pdeA*	*Bb*9.73H$^+$ wild-type strain with p*pdeA*	This work

expression of many virulence factors, such as iron-related proteins, adhesins, and the TTSS, by still-unknown mechanisms. Of note, we describe c-di-GMP-mediated regulation from an unregulated situation: artificially high or low c-di-GMP levels were used. It is expected that in a normal physiological situation, each DGC or PDE, at a certain moment, will activate or repress a group of proteins, corresponding to a specific phenotype. How *B. bronchiseptica* detects the appropriate time to activate a particular c-di-GMP network is a topic that needs further investigation.

MATERIALS AND METHODS

Protein structure prediction. Prediction was performed with Alphafold software using Colab interphase (54).

Bacterial strains and growth conditions. Strains and plasmids used in this study are listed in Table 1. *B. bronchiseptica* was grown routinely on Bordet-Gengou agar (Difco) supplemented with 15% defibrinated fresh sheep blood (BGA) at 37°C for 48 h. Hemolytic colonies were selected, restreaked onto another BGA plate, and incubated for 24 h at 37°C. When needed, Stainer-Scholte (SS) liquid medium was used to grow *B. bronchiseptica* (23). When appropriate, BGA and SS medium were supplemented with gentamicin (50 μg mL^{-1}).

A plasmid expressing *bb2664* (*pdeA*) was constructed as described previously using pBBR1MCS-5-p*nptII* as the backbone plasmid (16). As previously reported, *bb2664* was difficult to amplify by PCR, probably due to its high GC content (13). We designed two pairs of primers to amplify 5′ 759-bp and 3′ 853-bp oligonucleotide fragments with overlapping sequences (Table S3; Fig. S5). Both PCR products were mixed with pMQ72 plasmid, and recombination was allowed with the yeast cloning system (55). The final plasmid obtained was confirmed by sequencing. The complete *bb2664* gene was excised by digestion with EcoRI and HindIII and introduced in pBBR1MCS-5-p*nptII* by ligase reaction to obtain p*pdeA*.

B. bronchiseptica strains harboring plasmids were obtained by conjugation between wild-type *B. bronchiseptica* and *E. coli* S17-1 carrying the plasmids. Transformants were selected on BGA supplemented with streptomycin (200 μg mL^{-1}) and gentamicin (50 μg mL^{-1}).

***In vitro* PDE activity assays.** *B. bronchiseptica* strains carrying pEmpty or p*pdeA* overexpression plasmids were grown in SS liquid medium at 37°C overnight. Cultures were harvested by centrifugation at 4,500 $\times$ *g* for 15 min and resuspended in phosphate-buffered saline (PBS) with 1 mM phenylmethylsulfonyl fluoride (PMSF) and 500 mg of 0.1-mm glass beads. Cells were lysed by disruption at 6,500 rpm using 2 cycles of 20 s each on a Precellys 24 homogenizer (Bertin Instruments) and then centrifuged at 9,000 $\times$ *g* for 20 min at 4°C. The supernatant (crude cell extract) was used in PDE activity assays as described previously using the synthetic substrate bis-(*p*-nitrophenyl) phosphate (bis-*p*NPP) (56). A volume of 80 μL of crude cell extract was incubated for 60 min at 37°C in a 400-μL reaction mixture containing 50 mM Tris-HCl (pH 7.5), 20 mM $MgCl_2$, and 5 mM bis-*p*NPP. The release of *p*-nitrophenol was quantified at 410 nm in a spectrophotometer. The protein concentration in crude cell extract was determined with a standard Bradford reagent assay (Bio-Rad). Activity means were analyzed for significance using a one-way analysis of variance (ANOVA) with Tukey's multiple-comparison test to compare differences among groups. A Shapiro-Wilks test was performed to confirm normal distribution of data. Significance levels are stated in the figure legends.

Biofilm assays. *B. bronchiseptica* biofilm assays were performed as previously described by our group (16). Briefly, bacteria were resuspended in SS liquid medium to an optical density at 650 nm (OD_{650}) of 0.1, pipetted into a sterile 96-well U-bottom microtiter plate (polyvinylchloride), and incubated statically at 37°C for 24 h. After incubation, attached cells were stained with 0.1% (wt/vol) crystal violet solution. After a 30-min incubation, the solution was removed, and the plate was rinsed with deionized water. The remaining biofilm-associated stain was dissolved by adding 120 μL of 33% acetic acid solution and then quantified by measuring absorbance at 595 nm. Experiments were repeated with a minimum of 3 biological replicates and 6 technical replicates. Means were analyzed for significance using a one-way ANOVA with Tukey's multiple-comparison test to compare differences among groups. A

Shapiro-Wilks test was performed to confirm normal distribution of data. Significance levels are stated in the figure legends.

Sample preparation for proteomic analysis. *B. bronchiseptica* was cultivated in SS medium supplemented with appropriate antibiotics at 37°C and incubated with shaking at 160 rpm for 18 h. Cells were collected by centrifugation (9,000 × *g*, 20 min) and resuspended in buffer (10 mM $MgCl_2$, 20 mM Tris-HCl [pH 8.0]). Cells were disrupted using glass beads on a Precellys 24 homogenizer as described above. The intact cells were removed by centrifugation (10,000 × *g*; 30 min; 4°C), and the supernatant was retained. The samples were next centrifuged (100,000 × *g*; 1 h; 4°C). The resulting supernatant, enriched in cytosolic proteins, was subjected to DNase and RNase treatment and concentrated by acetone precipitation. Samples were stored at −80°C until trypsinization.

Orbitrap procedure. Samples were resuspended to a final protein concentration of 1 mg mL^{-1} in 50 mM ammonium bicarbonate, pH 8.0, and were reduced with dithiothreitol (40 mM in 50 mM ammonium bicarbonate) at 56°C for 60 min and then alkylated with freshly prepared iodoacetamide (22 mM in 50 mM ammonium bicarbonate) at room temperature in the dark for 60 min. Samples were digested overnight at 37°C with a final concentration of 2 ng mL^{-1} trypsin (Promega V5111). Peptides were desalted with ZipTip C_{18} columns (Millipore) and resuspended in 12 μL of 0.1% formic acid in water. Three independent biological replicates for each strain were analyzed.

Aliquots of samples were injected onto an Easy-Spray PepMap rapid-separation liquid chromatography (RSLC) column (Thermo Scientific) (2 μm, 100 Å, 75 μm by 500 mm) coupled to a Q-Exactive mass spectrometer (Thermo Scientific) and Orbitrap analyzer. The flow rate used for the nano column was 300 nl min^{-1}, and the solvent range was from 7% B (5 min) to 35% (240 min). Solvent A was 0.1% formic acid in water, whereas B was 0.1% formic acid in acetonitrile. The injection volume was 2 μL. Online mass spectrometry (MS) analysis was carried out in a data-dependent mode. Full-scan mass spectra were acquired in the Orbitrap analyzer. The scanned mass range was 400 to 1,800 *m/z*, at a resolution of 70,000 at 400 *m/z*, and the 12 most intense ions in each cycle were sequentially isolated (using a dynamic exclusion list), fragmented by high-energy collisional dissociation (HCD) and measured in the Orbitrap analyzer. Peptides with a charge of +1 or with an unassigned charge state were excluded from fragmentation for MS2.

The raw files obtained from Orbitrap MS/MS were imported into the label-free quantification (LFQ) MaxQuant search engine. For protein identification in MaxQuant, the database search engine Andromeda was used to search MS/MS spectra against the *B. bronchiseptica* RB50 proteome downloaded from the UniProt database (UP000001027), with a tolerance level of 6 ppm for MS and 20 ppm for MS/MS. Trypsin/P was set as the enzyme, and a maximum of two missed cleavages was allowed. Protein N-terminal acetylation and oxidation of methionines were set as variable modifications, and carbamidomethylation of cysteines was set as a fixed modification. The default setting was used for all other configurations.

Protein processing and Orbitrap data acquisition were performed by the Center of Chemical and Biological Studies by Mass Spectrometry (Centro de Estudios Químicos y Biológicos por Espectrometría de Masa [CEQUIBIEM], National University of Buenos Aires). Raw data were analyzed using the Maxquant software (version 1.5.3.30). Statistical analysis of MaxQuant output was performed by Perseus software (version1.5.6.0; Max Planck Institute, Germany) (57, 58).

RNA isolation and RNA-seq. *B. bronchiseptica* grown in SS medium as described above was pelleted by 13,000 rpm for 30 s, and supernatant was discarded. The pellet was resuspended in RNAprotect bacterial reagent (Qiagen) and centrifuged at 14,000 rpm for 3 min, and pellets were stored at −80°C. Three biological replicates were prepared for each strain.

RNA isolation was performed using the RNA snap method as described by Stead et al. and adapted for RNA sequencing by Damron et al. (59, 60). Briefly, cell pellets were resuspended in RNA extraction solution (18 mM EDTA, 0.025% SDS, 1% 2-mercaptoethanol, 95% formamide) by vortexing vigorously, incubated at 95°C for 7 min for cell lysis, and pelleted by centrifugation at 16,000 × *g* for 5 min at room temperature. The supernatant containing RNA was pipetted into a fresh tube, and RNA was then purified using an RNeasy minikit (Qiagen) as specified by the manufacturer's instructions.

To remove contaminating DNA, the samples were treated with a Turbo DNA-free kit (Ambion), according to the manufacturer's instructions for rigorous DNase treatment, and the RNA was reisolated with another RNeasy column. RNA concentration was measured using a Qubit 3.0 fluorometer, and the samples were confirmed as being DNA free by RT-qPCR amplification (with *recA* specific primers) (Table S3).

Total RNA was treated with the Ribo-Zero kit (Illumina) for rRNA depletion, and the libraries were prepared using ScriptSeq (Illumina). The libraries were sequenced on an Illumina HiSeq instrument at the Marshall University Genomics Core facility (Huntington, WV, USA).

RNA-seq analysis was performed using CLC Genomics Workbench 9.5.4. A total of 25 million 2 × 150-bp reads were devoted to each sample. All reads were trimmed based on quality scores with standard settings and mapped to the *B. bronchiseptica* RB50 reference genome (RefSeq no. NC_002927.3). Only paired reads were counted toward expression analysis. Genes displayed were filtered such that they must be significant (EDGE test, P value < 0.05) compared to the wild type.

RT-qPCR. cDNA was synthesized using Moloney murine leukemia virus (M-MLV) reverse transcriptase (Promega) according to manufacturer's instructions, using 500 ng of RNA and gene-specific reverse primers for each target. All primers used are listed in Table S3. qPCR mixtures were set up with Excella SYBR green PCR master mix (Worldwide Medical Products), per the manufacturer's instructions, using 1 μL of cDNA. Three technical replicate reactions were run per target gene per sample on a Step One Plus qPCR thermocycler (Applied Biosystems). Primers were designed on Primer3 and checked for specificity by PCR (61). Gene expression was normalized with *recA*, which is constitutively expressed, using the $2^{-\Delta\Delta CT}$ method as described before (16). For statistical analysis, the difference in cycle

threshold (ΔC_T) of the three biological replicates with three technical replicates each was calculated and Student's *t* test was performed.

Western blotting. Overnight *B. bronchiseptica* cultures grown in SS medium with the appropriate antibiotics were harvested by centrifugation (9,000 × *g*; 20 min), and supernatants were recovered and filtered through a low-binding protein filter with a 0.22-μm pore size. Samples were concentrated with Amicon Ultra centrifugal filter (molecular weight cutoff [MWCO], 10 kDa), normalized according to culture OD_{650}, subjected to SDS-PAGE, and transferred onto polyvinylidene difluoride (PVDF) membranes by Western blotting. Proteins were detected on the membrane using polyclonal sera against Bsp22 kindly donated by M. E. Gaillard (62). Membrane-bound antibodies were detected using the Clarity Western enhanced chemiluminescence (ECL) substrate (Bio-Rad) and exposure to film (Blue XB-1; Kodak, Rochester, NY). Film images of Western blots were digitalized.

Cytotoxicity assay. Cytotoxicity assays were conducted on J774A.1 macrophage-like cells, using the Pierce LDH cytotoxicity assay kit (Thermo Scientific) and following the manufacturer's protocols. J774A.1 macrophages were grown in Dulbecco's modified Eagle medium (DMEM) supplemented with 10% fetal bovine serum (FBS) and 1% penicillin-streptomycin, in 5% CO_2 at 37°C. A total of 10^4 cells were seeded in triplicate in 96-well plates. Bacteria were grown overnight in SS liquid medium with shaking at 160 rpm at 37°C, diluted with DMEM with 10% FBS, and added to the cells at multiplicities of infection (MOI) of 10:1 and 100:1. The plates were centrifuged at 300 × *g* for 5 min and then incubated for 4 h in 5% CO_2 at 37°C. *P* values were calculated using an unpaired one-tailed Student's *t* test.

Murine respiratory infection model. Five-week-old outbred CD1 mice were used as a model for *in vivo* respiratory infection by *B. bronchiseptica*. Bacteria grown overnight on SS medium at 36°C were diluted to provide a challenge dose of 10^6 CFU/20 μL. Mice were anesthetized by intraperitoneal injection of ketamine (7.7 mg kg^{-1}) and xylazine (0.77 mg kg^{-1}) in 0.9% saline, and 10 μL of the bacterial suspension was pipetted directly into each nostril. At days 1, 4, and 7 postchallenge, four mice from each challenged group were euthanized. Euthanasia was performed by intraperitoneal injection of pentobarbital.

Cardiac puncture was performed to collect blood. BD Microtainer tubes with K_2EDTA (BD) were used to collect blood for complete blood cell counts and flow cytometry. The hematology profiles were obtained using a Hemavet 950FS (Drew Scientific). Lungs, tracheas, and NALT were removed aseptically and homogenized for determination of the number of viable bacteria in those tissues. Lungs weights were recorded prior to homogenization. Lung homogenates were pelleted and the supernatants were collected and stored at −80°C for cytokine analysis. One milliliter of sterile PBS was used to flush mouse nares and collected for determination of bacterial burden. Serial dilutions in PBS of lung homogenate, trachea, nasal wash, and NALT were plated on BGA containing 200 μg/mL streptomycin for determination of viable bacteria and incubated for 3 days at 37°C. Duplicates were plated on BGA with 50 μg/mL gentamicin to confirm plasmid presence in bacteria. All murine infection experiments were performed according to protocols approved by the West Virginia University Animal Care and Use Committee (protocol no. 1602000797). Data were analyzed using GraphPad Prism 6, and comparisons between two groups were performed using an unpaired Student's *t* test.

Flow cytometry. Cells isolated from blood and lung homogenates were analyzed by flow cytometry. Lung homogenate samples were diluted in 4 mL of PBS, filtered through a 100-μm cell strainer, and centrifuged at 1,000 × *g* for 5 min to pellet cells. The cells were resuspended in red blood cell (RBC) lysis buffer (BD Pharm Lyse), incubated at 37°C for 2 min, and pelleted again. After the supernatant was discarded, cells were resuspended in PBS with 1% (vol/vol) FBS and Fc Block for Fc receptor blocking and incubated 15 min on ice. Cell suspensions were mixed with the antibody cocktails, incubated for 1 h at 4°C in the dark, washed, and finally resuspended in PBS. Blood collected in EDTA-containing tubes was treated with Pharm Lyse (BD) with a 15-min room temperature incubation to lyse red blood cells and then prepared for flow cytometry as described above. The antibodies used were phycoerythrin (PE)-conjugated Gr-1 and BB515-conjugated CD11b. After the incubation, the cells were washed with fluorescence-activated cell sorting (FACS) buffer (1% FBS in PBS) and resuspended in fixation buffer (0.4% paraformaldehyde) overnight at 4°C. Prior to running the samples, fixed cells were washed and resuspended in FACS buffer. Samples were processed using LSR Fortessa flow cytometer (BD Biosciences) and analyzed using FlowJo (FlowJo, LLC). The flow cytometry gating strategy for myeloid cells from murine lungs was adapted from the work of Zaynagetdinov et al. (63). Statistical analyses were performed using GraphPad Prism 6, and comparisons between groups were performed by one-way ANOVA followed by Tukey's multiple-comparison test.

Cytokine analysis. The cytokines concentrations in the lung's homogenates were determined by a quantitative survey analysis using the Meso Scale Discovery V-PLEX proinflammatory panel 1 mouse kit (IFN-γ, IL-1β, IL-2, IL-4, IL-5, IL-6, IL-10, IL-12p70, KC/GRO, and TNF-α) and the mouse IL-17 ultrasensitive kit, per the manufacturer's instructions. Statistical analyses were performed using GraphPad Prism 6, and comparisons between groups were performed by ANOVA followed by Tukey's multiple-comparison test.

Ethics statement. Animal work in this study was carried out in strict accordance with the recommendations in the *Guide for the Care and Use of Laboratory Animals* of the National Institutes of Health (64). The West Virginia University Institutional Animal Care and Use Committee (IACUC) approved the protocols and this research under the IACUC protocol 1602000797.

Data availability. The mapped reads are available at the Sequence Read Archive (SRA) under BioProject accession number PRJNA836179. Supplemental material is available for download at http://sedici.unlp.edu.ar/handle/10915/135429.

ACKNOWLEDGMENTS

We are grateful to Paula Giménez and Silvana Tongiani (both members of CPA CONICET at IBBM) and to María Pía Valacco, Jorge Germán Fernández, and Silvia Margarita Moreno

for the excellent support at the CEQUIBIEM. We are grateful to Mariette Barbier, Justin Bevere, and Jesse Hall for their review of the manuscript.

Conceptualization: M.D.L.P.G., J.F., and F.S. M.D.L.P.G. participated in all experiments. M.P.G. and T.Y.W. performed mouse experiments. M.D.L.P.G. performed cytotoxicity assays. F.S. and J.F. conducted the Orbitrap data analysis. M.D.L.P.G. conducted the RNA-seq data analysis. Writing original draft: M.D.L.P.G., F.S., and J.F. Writing – Review & editing: F.S., J.F., and F.H.D. Funding acquisition: F.H.D., F.S., and J.F. All authors contributed to the discussion and provided comments on the manuscript. All authors gave approval for the final version of the manuscript.

This work was supported by grants PICT-2016-0492 and PID-UNLP-X819 to J.F. and F.S. F.S. and J.F. are members of the Research Career of CONICET. M.D.L.P.G. is a fellow of UNLP. This project was also supported by NIH R01AI137155 to F.H.D. Flow cytometry experiments were performed in the West Virginia University Flow Cytometry Core Facility, which is supported by a TME CoBRE GM121322 grant and by the National Institutes of Health equipment grant S10OD016165 and the Institutional Development Award (IDeA) from the National Institute of General Medical Sciences of the National Institutes of Health under grant numbers P30GM103488 (CoBRE) and P20GM103434 (INBRE). F.H.D. is also funded by the Vaccine Development center at WVU-HSC through a Research Challenge Grant (no. HEPC.dsr.18.6) from the Division of Science and Research, WV Higher Education Policy Commission.

REFERENCES

1. Kirimanjeswara GS, Agosto LM, Kennett MJ, Bjornstad ON, Harvill ET. 2005. Pertussis toxin inhibits neutrophil recruitment to delay antibody-mediated clearance of Bordetella pertussis. J Clin Invest 115:3594–3601. https://doi.org/10.1172/JCI24609.
2. Parkhill J, Sebaihia M, Preston A, Murphy LD, Thomson N, Harris DE, Holden MTG, Churcher CM, Bentley SD, Mungall KL, Cerdeño-Tárraga AM, Temple L, James K, Harris B, Quail MA, Achtman M, Atkin R, Baker S, Basham D, Bason N, Cherevach I, Chillingworth T, Collins M, Cronin A, Davis P, Doggett J, Feltwell T, Goble A, Hamlin N, Hauser H, Holroyd S, Jagels K, Leather S, Moule S, Norberczak H, O'Neil S, Ormond D, Price C, Rabbinowitsch E, Rutter S, Sanders M, Saunders D, Seeger K, Sharp S, Simmonds M, Skelton J, Squares R, Squares S, Stevens K, Unwin L, et al. 2003. Comparative analysis of the genome sequences of Bordetella pertussis, Bordetella parapertussis and Bordetella bronchiseptica. Nat Genet 35:32–40. https://doi.org/10.1038/ng1227.
3. van Gent M, Heuvelman CJ, van der Heide HG, Hallander HO, Advani A, Guiso N, Wirsing von Kőnig CH, Vestrheim DF, Dalby T, Fry NK, Pierard D, Detemmerman L, Zavadilova J, Fabianova K, Logan C, Habington A, Byrne M, Lutyńska A, Mosiej E, Pelaz C, Gröndahl-Yli-Hannuksela K, Barkoff AM, Mertsola J, Economopoulou A, He Q, Mooi FR. 2015. Analysis of Bordetella pertussis clinical isolates circulating in European countries during the period 1998–2012. Eur J Clin Microbiol Infect Dis 34:821–830. https://doi.org/10.1007/s10096-014-2297-2.
4. Hewlett EL, Burns DL, Cotter PA, Harvill ET, Merkel TJ, Quinn CP, Stibitz ES. 2014. Pertussis pathogenesis—what we know and what we don't know. J Infect Dis 209:982–985. https://doi.org/10.1093/infdis/jit639.
5. Mattoo S, Foreman-Wykert AK, Cotter PA, Miller JF. 2001. Mechanisms of Bordetella pathogenesis. Front Biosci 6:E168–E186. https://doi.org/10.2741/mattoo.
6. Irie Y, Mattoo S, Yuk MH. 2004. The Bvg virulence control system regulates biofilm formation in Bordetella bronchiseptica. J Bacteriol 186:5692–5698. https://doi.org/10.1128/JB.186.17.5692-5698.2004.
7. Akerley BJ, Monack DM, Falkow S, Miller JF. 1992. The bvgAS locus negatively controls motility and synthesis of flagella in Bordetella bronchiseptica. J Bacteriol 174:980–990. https://doi.org/10.1128/jb.174.3.980-990.1992.
8. Ruhal R, Antti H, Rzhepishevska O, Boulanger N, Barbero DR, Wai SN, Uhlin BE, Ramstedt M. 2015. A multivariate approach to correlate bacterial surface properties to biofilm formation by lipopolysaccharide mutants of Pseudomonas aeruginosa. Colloids Surf B Biointerfaces 127:182–191. https://doi.org/10.1016/j.colsurfb.2015.01.030.
9. Cotter PA, Jones AM. 2003. Phosphorelay control of virulence gene expression in Bordetella. Trends Microbiol 11:367–373. https://doi.org/10.1016/s0966-842x(03)00156-2.
10. Martinez de Tejada G, Cotter PA, Heininger U, Camilli A, Akerley BJ, Mekalanos JJ, Miller JF. 1998. Neither the Bvg$^-$ phase nor the vrg6 locus of Bordetella pertussis is required for respiratory infection in mice. Infect Immun 66:2762–2768. https://doi.org/10.1128/IAI.66.6.2762-2768.1998.
11. Bibova I, Skopova K, Masin J, Cerny O, Hot D, Sebo P, Vecerek B. 2013. The RNA chaperone Hfq is required for virulence of Bordetella pertussis. Infect Immun 81:4081–4090. https://doi.org/10.1128/IAI.00345-13.
12. Barbier M, Boehm DT, Sen-Kilic E, Bonnin C, Pinheiro T, Hoffman C, Gray M, Hewlett E, Damron FH. 2017. Modulation of pertussis and adenylate cyclase toxins by sigma factor RpoE in Bordetella pertussis. Infect Immun 85:e00565-16. https://doi.org/10.1128/IAI.00565-16.
13. Kaut CS, Duncan MD, Kim JY, Maclaren JJ, Cochran KT, Julio SM. 2011. A novel sensor kinase is required for Bordetella bronchiseptica to colonize the lower respiratory tract. Infect Immun 79:3216–3228. https://doi.org/10.1128/IAI.00005-11.
14. Coutte L, Huot L, Antoine R, Slupek S, Merkel TJ, Chen Q, Stibitz S, Hot D, Locht C. 2016. The multifaceted RisA regulon of Bordetella pertussis. Sci Rep 6:32774. https://doi.org/10.1038/srep32774.
15. Guragain M, Jennings-Gee J, Cattelan N, Finger M, Conover MS, Hollis T, Deora R. 2018. The transcriptional regulator BpsR controls the growth of Bordetella bronchiseptica by repressing genes involved in nicotinic acid degradation. J Bacteriol 200:e00712-17. https://doi.org/10.1128/JB.00712-17.
16. Sisti F, Ha D-G, O'Toole GA, Hozbor D, Fernández J. 2013. Cyclic-di-GMP signalling regulates motility and biofilm formation in Bordetella bronchiseptica. Microbiology (Reading) 159:869–879. https://doi.org/10.1099/mic.0.064345-0.
17. Belhart K, Gutierrez M. d l P, Zacca F, Ambrosis N, Cartelle Gestal M, Taylor D, Dahlstrom KM, Harvill ET, O'Toole GA, Sisti F, Fernández J. 2019. *Bordetella bronchiseptica* diguanylate cyclase BdcA regulates motility and is important for the establishment of respiratory infection in mice. J Bacteriol 201:e00011-19. https://doi.org/10.1128/JB.00011-19.
18. Hall CL, Lee VT. 2018. Cyclic-di-GMP regulation of virulence in bacterial pathogens. Wiley Interdiscip Rev RNA 9:e1454. https://doi.org/10.1002/wrna.1454.
19. Römling U, Liang Z-X, Dow JM. 2017. Progress in understanding the molecular basis underlying functional diversification of cyclic dinucleotide turnover proteins. J Bacteriol 199:e00790-16. https://doi.org/10.1128/JB.00790-16.
20. Liu X, Beyhan S, Lim B, Linington RG, Yildiz FH. 2010. Identification and characterization of a phosphodiesterase that inversely regulates motility and biofilm formation in Vibrio cholerae. J Bacteriol 192:4541–4552. https://doi.org/10.1128/JB.00209-10.

21. Tchigvintsev A, Xu X, Singer A, Chang C, Brown G, Proudfoot M, Cui H, Flick R, Anderson WF, Joachimiak A, Galperin MY, Savchenko A, Yakunin AF. 2010. Structural insight into the mechanism of c-di-GMP hydrolysis by EAL domain phosphodiesterases. J Mol Biol 402:524–538. https://doi.org/10.1016/j.jmb.2010.07.050.
22. Nicholson TL, Conover MS, Deora R. 2012. Transcriptome profiling reveals stage-specific production and requirement of flagella during biofilm development in Bordetella bronchiseptica. PLoS One 7:e49166. https://doi.org/10.1371/journal.pone.0049166.
23. Stainer DW, Scholte MJ. 1970. A simple chemically defined medium for the production of phase I Bordetella pertussis. J Gen Microbiol 63:211–220. https://doi.org/10.1099/00221287-63-2-211.
24. Lesniak J, Barton WA, Nikolov DB. 2003. Structural and functional features of the Escherichia coli hydroperoxide resistance protein OsmC. Protein Sci 12:2838–2843. https://doi.org/10.1110/ps.03375603.
25. Huang CJ, Wang ZC, Huang HY, Huang HD, Peng HL. 2013. YjcC, a c-di-GMP phosphodiesterase protein, regulates the oxidative stress response and virulence of Klebsiella pneumoniae CG43. PLoS One 8:e66740. https://doi.org/10.1371/journal.pone.0066740.
26. Xiao Y, Zhu W, He M, Nie H, Chen W, Huang Q. 2019. High c-di-GMP promotes expression of fpr-1 and katE involved in oxidative stress resistance in Pseudomonas putida KT2440. Appl Microbiol Biotechnol 103:9077–9089. https://doi.org/10.1007/s00253-019-10178-6.
27. Johnson RM, Nash ZM, Dedloff MR, Shook JC, Cotter PA. 2021. DegP Initiates regulated processing of filamentous hemagglutinin in Bordetella bronchiseptica. mBio 12:e01465-21. https://doi.org/10.1128/mBio.01465-21.
28. Weng Y, Chen F, Liu Y, Zhao Q, Chen R, Pan X, Liu C, Cheng Z, Jin S, Jin Y, Wu W. 2016. Pseudomonas aeruginosa Enolase Influences Bacterial Tolerance to Oxidative Stresses and Virulence. Front Microbiol 7:1999. https://doi.org/10.3389/fmicb.2016.01999.
29. Nash ZM, Cotter PA. 2019. Regulated, sequential processing by multiple proteases is required for proper maturation and release of Bordetella filamentous hemagglutinin. Mol Microbiol 112:820–836. https://doi.org/10.1111/mmi.14318.
30. Finn TM, Stevens LA. 1995. Tracheal colonization factor: a Bordetella pertussis secreted virulence determinant. Mol Microbiol 16:625–634. https://doi.org/10.1111/j.1365-2958.1995.tb02425.x.
31. Sisti F, Fernández J, Rodríguez ME, Lagares A, Guiso N, Hozbor DF. 2002. In vitro and in vivo characterization of a Bordetella bronchiseptica mutant strain with a deep rough lipopolysaccharide structure. Infect Immun 70:1791–1798. https://doi.org/10.1128/IAI.70.4.1791-1798.2002.
32. Bokhari H, Bilal I, Zafar S. 2012. BapC autotransporter protein of Bordetella pertussis is an adhesion factor. J Basic Microbiol 52:390–396. https://doi.org/10.1002/jobm.201100188.
33. Glaser P, Sakamoto H, Bellalou J, Ullmann A, Danchin A. 1988. Secretion of cyclolysin, the calmodulin-sensitive adenylate cyclase-haemolysin bifunctional protein of Bordetella pertussis. EMBO J 7:3997–4004. https://doi.org/10.1002/j.1460-2075.1988.tb03288.x.
34. Herbst S, Lorkowski M, Sarenko O, Nguyen TKL, Jaenicke T, Hengge R. 2018. Transmembrane redox control and proteolysis of PdeC, a novel type of c-di-GMP phosphodiesterase. EMBO J 37:e97825. https://doi.org/10.15252/embj.201797825.
35. Dahlstrom KM, Collins AJ, Doing G, Taroni JN, Gauvin TJ, Greene CS, Hogan DA, O'Toole GA. 2018. A multimodal strategy used by a large c-di-GMP network. J Bacteriol 200:e00703-17. https://doi.org/10.1128/JB.00703-17.
36. Yuk MH, Harvill ET, Miller JF. 1998. The BvgAS virulence control system regulates type III secretion in Bordetella bronchiseptica. Mol Microbiol 28:945–959. https://doi.org/10.1046/j.1365-2958.1998.00850.x.
37. Ambrosis N, Boyd CD, O'Toole GA, Fernández J, Sisti F. 2016. Homologs of the LapD-LapG c-di-GMP effector system control biofilm formation by Bordetella bronchiseptica. PLoS One 11:e0158752. https://doi.org/10.1371/journal.pone.0158752.
38. Nagamatsu K, Kuwae A, Konaka T, Nagai S, Yoshida S, Eguchi M, Watanabe M, Mimuro H, Koyasu S, Abe A. 2009. Bordetella evades the host immune system by inducing IL-10 through a type III effector, BopN. J Exp Med 206:3073–3088. https://doi.org/10.1084/jem.20090494.
39. Brickman TJ, Suhadolc RJ, McKelvey PJ, Armstrong SK. 2017. Essential role of Bordetella NadC in a quinolinate salvage pathway for NAD biosynthesis. Mol Microbiol 103:423–438. https://doi.org/10.1111/mmi.13566.
40. Stockbauer KE, Fuchslocher B, Miller JF, Cotter PA. 2001. Identification and characterization of BipA, a Bordetella Bvg-intermediate phase protein. Mol Microbiol 39:65–78. https://doi.org/10.1046/j.1365-2958.2001.02191.x.
41. Hiramatsu Y, Saito M, Otsuka N, Suzuki E, Watanabe M, Shibayama K, Kamachi K. 2016. BipA is associated with preventing autoagglutination and promoting biofilm formation in Bordetella holmesii. PLoS One 11:e0159999. https://doi.org/10.1371/journal.pone.0159999.
42. Ahmad I, Lamprokostopoulou A, Le Guyon S, Streck E, Barthel M, Peters V, Hardt WD, Römling U. 2011. Complex c-di-GMP signaling networks mediate transition between virulence properties and biofilm formation in Salmonella enterica serovar Typhimurium. PLoS One 6:e28351. https://doi.org/10.1371/journal.pone.0028351.
43. Lamprokostopoulou A, Monteiro C, Rhen M, Römling U. 2010. Cyclic di-GMP signalling controls virulence properties of Salmonella enterica serovar Typhimurium at the mucosal lining. Environ Microbiol 12:40–53. https://doi.org/10.1111/j.1462-2920.2009.02032.x.
44. Moscoso JA, Mikkelsen H, Heeb S, Williams P, Filloux A. 2011. The Pseudomonas aeruginosa sensor RetS switches type III and type VI secretion via c-di-GMP signalling. Environ Microbiol 13:3128–3138. https://doi.org/10.1111/j.1462-2920.2011.02595.x.
45. Aragon IM, Pérez-Mendoza D, Moscoso JA, Faure E, Guery B, Gallegos MT, Filloux A, Ramos C. 2015. Diguanylate cyclase DgcP is involved in plant and human Pseudomonas spp. infections. Environ Microbiol 17:4332–4351. https://doi.org/10.1111/1462-2920.12856.
46. Yi X, Yamazaki A, Biddle E, Zeng Q, Yang CH. 2010. Genetic analysis of two phosphodiesterases reveals cyclic diguanylate regulation of virulence factors in Dickeya dadantii. Mol Microbiol 77:787–800. https://doi.org/10.1111/j.1365-2958.2010.07246.x.
47. Yuk MH, Harvill ET, Cotter PA, Miller JF. 2000. Modulation of host immune responses, induction of apoptosis and inhibition of NF-kappaB activation by the Bordetella type III secretion system. Mol Microbiol 35:991–1004. https://doi.org/10.1046/j.1365-2958.2000.01785.x.
48. Fennelly NK, Sisti F, Higgins SC, Ross PJ, Van Der Heide H, Mooi FR, Boyd A, Mills KHG. 2008. Bordetella pertussis expresses a functional type III secretion system that subverts protective innate and adaptive immune responses. Infect Immun 76:1257–1266. https://doi.org/10.1128/IAI.00836-07.
49. Kurushima J, Kuwae A, Abe A. 2012. Btc22 chaperone is required for secretion and stability of the type III secreted protein Bsp22 in Bordetella bronchiseptica. FEMS Microbiol Lett 331:144–151. https://doi.org/10.1111/j.1574-6968.2012.02561.x.
50. Ahuja U, Shokeen B, Cheng N, Cho Y, Blum C, Coppola G, Miller JF. 2016. Differential regulation of type III secretion and virulence genes in Bordetella pertussis and Bordetella bronchiseptica by a secreted anti-σ factor. Proc Natl Acad Sci U S A 113:2341–2348. https://doi.org/10.1073/pnas.1600320113.
51. Nishimura R, Abe A, Sakuma Y, Kuwae A. 2018. Bordetella bronchiseptica Bcr4 antagonizes the negative regulatory function of BspR via its role in type III secretion. Microbiol Immunol 62:743–754. https://doi.org/10.1111/1348-0421.12659.
52. Mahon BP, Ryan M, Griffin F, Mills KH. 1997. Mechanisms of immunity to the respiratory pathogen Bordetella pertussis in normal and gene knockout mice: clearance of primary infection is not enhanced by therapeutic interleukin-12. Biochem Soc Trans 25:341S. https://doi.org/10.1042/bst025341s.
53. Zogaj X, Wyatt GC, Klose KE. 2012. Cyclic di-GMP stimulates biofilm formation and inhibits virulence of Francisella novicida. Infect Immun 80:4239–4247. https://doi.org/10.1128/IAI.00702-12.
54. Mirdita M, Schütze K, Moriwaki Y, Heo L, Ovchinnikov S, Steinegger M. 2022. ColabFold—making protein folding accessible to all. bioRxiv. https://doi.org/10.1101/2021.08.15.456425.
55. Shanks RMQ, Caiazza NC, Hinsa SM, Toutain CM, O'Toole GA. 2006. Saccharomyces cerevisiae-based molecular tool kit for manipulation of genes from gram-negative bacteria. Appl Environ Microbiol 72:5027–5036. https://doi.org/10.1128/AEM.00682-06.
56. Bobrov AG, Kirillina O, Perry RD. 2005. The phosphodiesterase activity of the HmsP EAL domain is required for negative regulation of biofilm formation in Yersinia pestis. FEMS Microbiol Lett 247:123–130. https://doi.org/10.1016/j.femsle.2005.04.036.
57. Tyanova S, Temu T, Sinitcyn P, Carlson A, Hein MY, Geiger T, Mann M, Cox J. 2016. The Perseus computational platform for comprehensive analysis of (prote)omics data. Nat Methods 13:731–740. https://doi.org/10.1038/nmeth.3901.
58. Tyanova S, Temu T, Cox J. 2016. The MaxQuant computational platform for mass spectrometry-based shotgun proteomics. Nat Protoc 11:2301–2319. https://doi.org/10.1038/nprot.2016.136.
59. Damron FH, Oglesby-Sherrouse AG, Wilks A, Barbier M. 2016. Dual-seq transcriptomics reveals the battle for iron during Pseudomonas aeruginosa acute murine pneumonia. Sci Rep 6:39172. https://doi.org/10.1038/srep39172.

60. Stead MB, Agrawal A, Bowden KE, Nasir R, Mohanty BK, Meagher RB, Kushner SR. 2012. RNAsnap™: a rapid, quantitative and inexpensive, method for isolating total RNA from bacteria. Nucleic Acids Res 40:e156. https://doi.org/10.1093/nar/gks680.
61. Untergasser A, Cutcutache I, Koressaar T, Ye J, Faircloth BC, Remm M, Rozen SG. 2012. Primer3—new capabilities and interfaces. Nucleic Acids Res 40:e115. https://doi.org/10.1093/nar/gks596.
62. Gaillard ME, Bottero D, Castuma CE, Basile LA, Hozbor D. 2011. Laboratory adaptation of Bordetella pertussis is associated with the loss of type three secretion system functionality. Infect Immun 79:3677–3682. https://doi.org/10.1128/IAI.00136-11.
63. Zaynagetdinov R, Sherrill TP, Kendall PL, Segal BH, Weller KP, Tighe RM, Blackwell TS. 2013. Identification of myeloid cell subsets in murine lungs using flow cytometry. Am J Respir Cell Mol Biol 49:180–189. https://doi.org/10.1165/rcmb.2012-0366MA.
64. National Research Council. 2011. Guide for the care and use of laboratory animals, 8th ed. National Academies Press, Washington, DC.
65. Gueirard P, Weber C, Le Coustumier A, Guiso N. 1995. Human Bordetella bronchiseptica infection related to contact with infected animals: persistence of bacteria in host. J Clin Microbiol 33:2002–2006. https://doi.org/10.1128/jcm.33.8.2002-2006.1995.